Journal of
Composites Science

MDPI

Article

The Unstable Fracture of Multifilament Tows

Jacques Lamon

LMPS-ENS, Université Paris-Saclay, 4, Avenue des Sciences, CS 30008, 91192 Gif-sur-Yvette, France; jacques.lamon@ens-paris-saclay.fr

Abstract: The present paper investigates the unexpected unstable failure observed commonly on fiber tows tensile-tested under strain-controlled loading, although the force on the fibers should theoretically be relaxed under controlled strain. A model of the reaction of the load train when the fibers break under strain-controlled conditions is proposed. The criterion for instability is based on the comparison of the filament strength gradient and the overstress induced by the reaction of the load train when the fibers fail. The contribution of multiplet filament failures attributed to the fiber inter-friction and stress waves was taken into account. The compliance of the load train for the test results considered in the present paper was measured. It is shown that, depending on the number of filaments sharing the overload, the values of the structural parameters, and the fiber characteristics, the condition of unstable failure may have been fulfilled by the SiC fiber tows that were tested in house, as discussed in the present paper. The critical parameters that were identified and quantified include the load train compliance, gauge length, fiber stiffness, and bonding of the tow ends. This should allow the proper conditions for stable failure. Important implications for the validity and an analysis of the strengths derived from the unstable fracture of the tows are discussed.

Keywords: fibers; tows; fracture; strength

Citation: Lamon, J. The Unstable Fracture of Multifilament Tows. *J. Compos. Sci.* **2024**, *8*, 52. https://doi.org/10.3390/ jcs8020052

Academic Editor: Francesco Tornabene

Received: 7 November 2023
Revised: 18 December 2023
Accepted: 15 January 2024
Published: 30 January 2024

1. Introduction

In composites, fibers are fundamental constituents, as they carry nearly all the load in polymer matrix composites, as well as in ceramic matrix composites after the saturation of matrix damage. In multi-directionally reinforced composites, such as woven composites, fiber tows are the pertinent length scale for fracture analysis. For these reasons, the features of fiber tow fracture warrant much consideration with a view to composite failure analysis and prediction.

The fracture of a variety of materials is induced by inherent flaws that have random locations and severity [1–3]. The tensile strength of brittle fibers is a variate. As such, it is characterized by a statistical distribution. Reliable determination of the strength distribution requires a statistically representative set of measured strengths. The sample size effect is well documented in the literature (see, for instance, [4–9]). Testing on a bundle is a powerful approach to the determination of the filament strength statistical distribution, as it can provide as many data points as the number of filaments in the tow, i.e., hundreds or thousands of data points. Alternative determination of such a dataset on single filaments tested individually would require hundreds or thousands of tests, which would take weeks to months of careful test specimen preparation, testing, and analysis. For these reasons, testing a bundle of filaments as a whole is an attractive goal for many researchers [9–25], with a view to determining the fiber strength and lifetime at high temperatures.

The force–strain behavior of fiber tows is influenced by the testing conditions and the loading mode. Under the condition of a constant load, the load that was carried by the filament that breaks is shared by the surviving filaments (equal load sharing). Ultimate failure occurs when the surviving filaments are unable to carry the load increase.

Under quasi-static strain-controlled loading conditions (the strain rate is smaller than the damage kinetics), there is theoretically no overloading of the surviving fibers when a

fiber fails. The strain on the filaments is kept constant owing to the boundary conditions during the fiber break, and the force on the broken filament is relaxed according to the fracture mechanics. This effect is well illustrated by the experimental force–strain curves shown in Figure 1 [9], and by the typical force relaxation that was obtained experimentally on glass fibers under constant strain when the fiber failure was caused by stress corrosion [20].

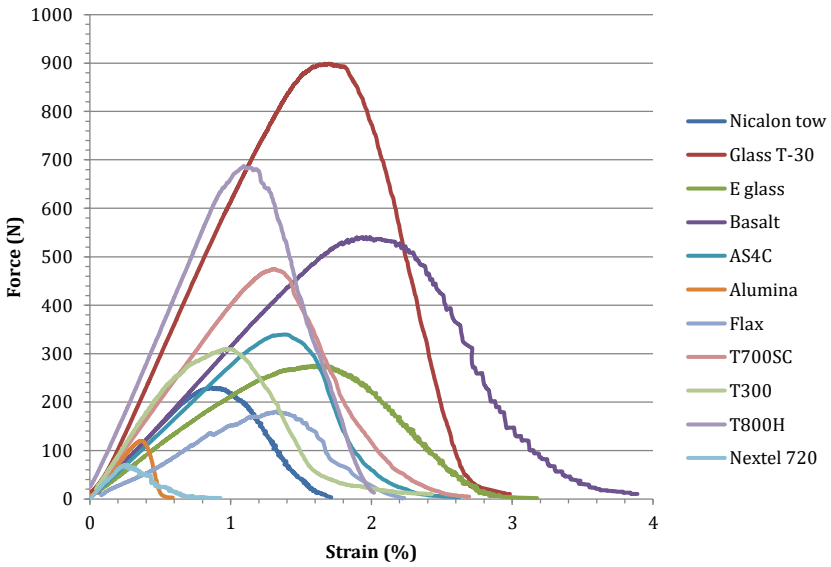

Figure 1. Typical force–strain curves with stable failure measured on various fiber tows [9].

Most laboratory tests are carried out under quasi-static mode and controlled strain. The following various types of force–strain behavior were commonly obtained on multifilament tows tested under strain-controlled loading:

(a) Stable failure associated with damageable elastic behavior resulting from the successive individual failure of filaments. The force–strain curve exhibits a remarkably stable and smooth load decrease beyond the maximum force to 0 (Figure 1). This behavior is well predicted by theory. It has been observed experimentally on several brittle fiber types, and it was shown that the corresponding filament strength distributions agree with the results of single-filament tensile tests [9].

(b) Stable premature tensile behavior with a progressive force decrease to 0. The filaments break successively under a lower applied force. This behavior has been reported by several authors on various fiber tow types (E-glass, carbon, SiC, Hi Nicalon S, and Kevlar) [15,21,23]. It was attributed to the damage induced by inter-fiber friction [15,21] and dynamic failure during breaking [11]. Numerical simulations of random fiber contacts showed that the force–strain behavior was affected by increasing fiber contacts, but the entire curve was retained [16]. Tests on lubricated and/or sized tows showed that the load-carrying capacity of tows was increased when compared with dry tows [15,21,22,25]. The lubricant and sizing reduce the lateral interactions between filaments. The friction between fibers was also evidenced on histograms of the amplitudes of acoustic emission signals [15]. When a filament breaks, it gets shorter and moves against the fibers that are touching it. Depending on the filament surface roughness, the induced tensile stresses may cause the failure of additional filaments. The related additional acoustic emission increases with gauge length [15,21]. Acoustic emission histograms also revealed that for short gauge lengths, the breaks are located near the bundle ends [15]. For larger gauge lengths, the end effect was reduced [15]. The end effects in carbon single-filament fiber tests have been examined in [26]. The contribution of end effects in the case of fiber tows has not been extensively studied in the literature.

(c) The unstable failure of tows is frequently observed. It occurs in an unpredictable manner close to the maximum load, although the force on the fibers should theoretically be relaxed under controlled strain. This fracture behavior requires an extra load that may result from structural effects such as inter-fiber friction, stress waves, and load train deformation in tows without slack.

The force–strain behavior is influenced by the testing conditions. Dry tows tested using the RMili technique [14] showed stable fracture behavior along with a smooth controlled load decrease beyond the maximum, as shown in Figure 1 [20]. The test specimen elongation was measured using a contact extensometer that was clamped to the specimen using two 4 mm long thermoretractable rings [14]. The other authors referred to above in (b) and (c) did not use this technique. The regions outside the fiber specimen gauge length were bonded to plates (aluminum or epoxy [21,22]) or tubes (this study) using adhesive.

The present paper investigates the paradoxical unstable failure of SiC fiber tows (described in section (c)) that were tested in-house under strain-controlled loading. A model of reloading involving the load train reaction when the fibers break and the inter-fiber friction is proposed. It allowed us to identify and quantify the parameters that controlled this phenomenon with a view to determining the proper conditions for stable failure and the determination of a pertinent tow strength.

2. Theory

2.1. Unstable Failure of Dry Tows

The bundle models are based upon the following hypotheses [10,12,16,24]: the bundle contains N_0 identical and parallel fibers that are equally loaded (equal load sharing). The loading conditions affect significantly the tensile behavior of dry tows.

(a) Under load-controlled conditions, the force on the tow is kept constant during filament breakage so that the force operating on the breaking filament is shared equally by the surviving filaments. The failure of a filament thus induces overloading on the surviving fibers by an increment

$$\Delta\sigma_{ai} = \frac{\sigma_{ai}}{N_0 - i} \tag{1}$$

where i designates the fiber that failed (according to ascending strength order) and σ_{ai} is the stress that operated on this fiber before failure. i designates also the corresponding number of broken fibers.

Unstable failure occurs when $\Delta\sigma_{ai} > \sigma_{i+1} - \sigma_i$ whatever the value of i is. σ_{i+1} is the strength of the fiber with a rank $i + 1$ in the cumulative distribution of strengths. This condition is expressed as:

$$\frac{d\sigma_a}{dP} \geq \frac{d\sigma}{dP} \tag{2}$$

where σ_a is the stress operating on the filaments under force-controlled load and σ is the filament strength. P is the failure probability. It has been shown in previous papers [9] that the cumulative distribution of SiC filament tensile strengths can be described using the Weibull distribution function [27]:

$$P_w(\Sigma < \sigma) = 1 - \exp\left[-\frac{V}{V_0}\left(\frac{\sigma}{\sigma_0}\right)^m\right] \qquad \text{for } \sigma > 0 \tag{3}$$

where m is the shape parameter (Weibull modulus) and σ_0 isthe scale factor, V is the stressed volume, and $V_0 = 1\ m^3$.

The filament strength is derived from Equation (3):

$$\sigma = \sigma_0\left[\frac{V_0}{V} Ln\left(\frac{1}{1-P}\right)\right]^{\frac{1}{m}} \tag{4}$$

The filament strength gradient in a tow is $\Delta\sigma = \frac{d\sigma}{dP}\Delta P$. From the derivation of Equation (4) comes:

$$\Delta\sigma = \frac{\sigma}{m(1-P)Ln\left(\frac{1}{1-P}\right)}\Delta P \quad (5)$$

When $\Delta P = 1/N_0$, N_0 being the initial number of filaments carrying the load, $\Delta\sigma$ measures the difference between two successive filament strengths of the cumulative distribution. The critical fiber in a tow for which Condition (2) is met is defined by the particular value of probability (α_c) in the cumulative distribution of the filament strengths. α_c corresponds to the maximum force of the tensile curve obtained under strain-controlled conditions.

$$P = \alpha_c = 1 - \exp\left(-\frac{1}{m}\right) \quad (6)$$

Figure 2 compares the stress increase $\Delta\sigma_a$ (Equation (1)) under a constant load with the strength gradient $\Delta\sigma$ in tow. It shows that under such a loading condition, $\Delta\sigma_a > \Delta\sigma$ for filament failure probabilities $P > 0.17$. It is worth pointing out that this value of P was also obtained using Equation (6) of α_c for a value of $m = 4.8$.

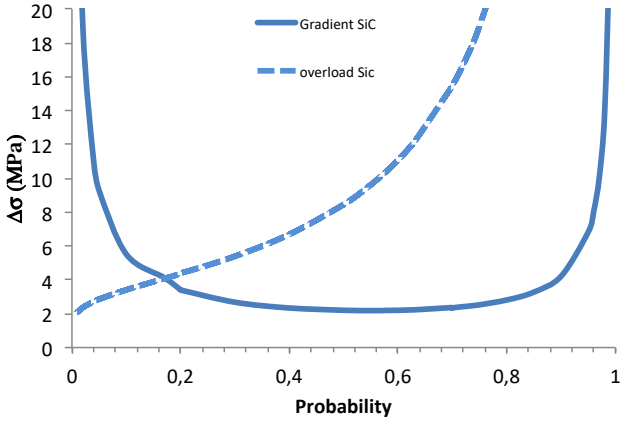

Figure 2. Gradient $\Delta\sigma$ of filament strengths in SiC Nicalon fiber tows vs. filament failure probability in strength distribution. Also shown is the stress increase in the surviving fibers $\Delta\sigma_a$ caused by the failure of a filament under constant force.

(b) Under *strain-controlled conditions*, there is theoretically no overloading of the surviving fibers from the failure of a filament since the strain on the filaments is kept constant by the boundary conditions during fiber breakage. This effect is well illustrated by the experimental results obtained on fiber tows (Figure 1): the tensile force–strain curves do not exhibit unstability until complete failure of the tow and show load relaxation. Load relaxation when a filament fails under constant deformation is demonstrated in the subsequent section.

Thus, $\Delta\sigma_a = 0$, and the condition of unstable failure is not fulfilled unless an extra load operates. It can be generated by an artifact such as the contribution of the load train deformation and inter-fiber friction.

2.2. Model of Reaction of the Load Train When Fibers Break under Strain-Controlled Conditions

Figure 3 describes the steps of the respective deformations of the tow and load train resulting from a filament failure under contant displacement. Under controlled displacement u of the cross-head of the testing machine, the elongations of the load train and tow are u_{Lt} and u_{tow}, respectively, such that $u = u_{LT} + u_{tow}$. The compliance of the tow increases with the decreasing number of filaments carrying the load, according to the equation:

$$C_{tow}(n) = \frac{u_{tow}}{F} = \frac{L_0\varepsilon_{tow}}{\sigma_f S_f n} \quad (7)$$

where n is the number of filaments carrying the load, F is the force operating on the test specimen, L_0 is the gauge length, ε_{tow} is the tow strain, σ_f is the stress on the filaments, and S_f is the filament's cross-sectional area.

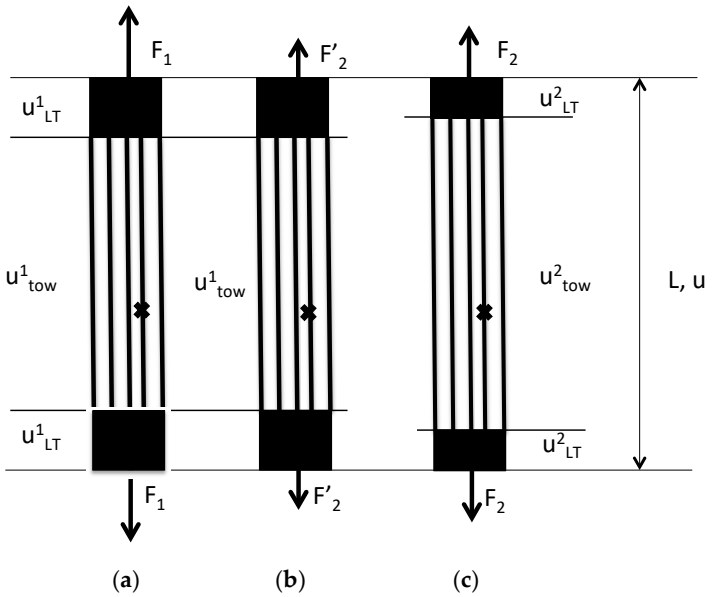

Figure 3. Sketch showing the steps of respective deformations of tow and load train resulting from filament failure under constant displacement u: (**a**) failure of a multifilament; (**b**) load relaxation at constant tow deformation $u^1{}_{tow}$; (**c**) reloading of tow from reaction of load train. The deformations defined in Equations (9) and (10) $u^1{}_{LT}$, $u^2{}_{LT}$, $u^1{}_{tow}$, $u^2{}_{tow}$ are not represented in the sketch.

Replacing σ_f with $E_f\,\varepsilon_{tow}$, Equation (7) reduces to:

$$C_{tow}(n) = \frac{L_0}{E_f S_f n} \tag{8}$$

When p filaments fail at constant deformation u (Figure 3),

$$u = u^1_{LT} + u^1_{tow} = u^2_{LT} + u^2_{tow} \tag{9}$$

$$u = C_{LT}F_1 + \frac{L_0F_1}{E_fS_fn} = C_{LT}F_2 + \frac{L_0F_2}{E_fS_f(n-p)} \tag{10}$$

where the subscripts 1 and 2 refer to the values before and after the failure of the p filaments, respectively. $p > 1$ when a multiplet is created due to the inter-fiber friction. C_{LT} is the compliance of the load train.

From the system of Equation (10), the force decrease (Figure 3) resulting from the p-filament failure (ΔF) at constant deformation is obtained as:

$$\Delta F = F_1 - F_2 = \frac{F_1L_0}{n(n-p)C_{LT}S_fE_f + L_0n} \tag{11}$$

The resulting force on the tow is:

$$F_2 = F_1\,\frac{n-p}{n}\,\frac{nC_{LT}S_fE_f + L_0}{(n-p)C_{LT}S_fE_f + L_0} \tag{12}$$

Equation (12) shows that F_2 depends essentially on the number of filaments and the parameter λ defined by Equation (13), which characterizes the contribution of the load train:

$$\lambda = \frac{C_{LT} S_f E_f}{L_0} \tag{13}$$

Introducing the equation of λ into Equation (12) gives the following equation of F_2.

$$F_2 = F_1 \frac{n-p}{n} \frac{1+\lambda n}{1+\lambda(n-p)} \tag{14}$$

In the case of an undeformable load train ($u_{LT} = 0$), the true force operating on the tow (F_2') (Figure 3) is determined from Equation (15), derived from Equations (9) and (10):

$$u = u_{tow} = \frac{L_0 F_1}{E_f S_f n} = \frac{L_0 F_2'}{E_f S_f (n-p)} \tag{15}$$

$$F_2' = F_1 \frac{n-p}{n} \tag{16}$$

where F_2' is the value of the force on the tow after the fracture of the p filaments at constant deformation.

Introducing Equation (16) of F_2', the following equation of F_2 is derived from Equation (14):

$$F_2 = F_2' \frac{1+\lambda n}{1+\lambda(n-p)} \tag{17}$$

Equation (17) shows that $F_2 > F_2'$, which indicates that the force operating after the failure of the p filaments is larger than the true force on tow F_2', which would operate in the absence of the deformation of the load train (Figure 3). The resulting overload that operates on the tow, F_{LT}, is a tensile force.

The force F_{LT} resulting from the contribution of the load train is derived from Equation (17).

$$F_{LT} = F_2 - F_2' = F_1 \frac{n-p}{n} \frac{\lambda p}{1+\lambda(n-p)} \tag{18}$$

Equation (18) shows that F_{LT} depends essentially on the number of filaments n and p and the parameter λ defined by Equation (13) that characterizes the contribution of the load train. λ depends also on the following filament characteristics: E_f, S_f, and L_0.

Thus, it has been established that an extra tensile load due to the contribution of the deformable load train can operate. This overload may be shared by one or several filaments: $1 \leq k \leq n$. The next step is to show whether this overload is able to induce unstable fracture of the tow.

2.3. Criterion for Unstability under Constant Deformation

The failure of the filaments occurs when the overstress increase $\Delta\sigma(k)$ on k filaments exceeds the stress gradient between filament i that failed and filament $i+1$. According to the above Condition (2) comes:

$$\Delta\sigma(k) = \frac{F_{LT}}{kS_f} \geq \Delta\sigma(\Delta P) \tag{19}$$

$$\frac{F_1}{nS_f} \frac{p\lambda(n-p)}{k(1+\lambda(n-p))} \geq \frac{\sigma\Delta P}{m(1-P)Ln\left(\frac{1}{1-P}\right)} \tag{20}$$

Knowing that $\sigma_a = \sigma = \frac{F_1}{nS_f}$, it comes from Condition (20) the following requirement for λ to avoid the failure of filaments by the overloading from the load train reaction:

$$\lambda \leq \frac{k\Gamma}{(n-p)(p-k\Gamma)} \tag{21}$$

where $\Gamma = \frac{\Delta P}{m(1-P)Ln\left(\frac{1}{1-P}\right)}$.

Note that Condition (21) depends on n, p, and k. The critical value λ^* of λ below which there is no contribution of the load train deformation whatever the values of n, p and k is given by the following equation:

$$\frac{d(\Delta\sigma(k))}{dP} = \frac{d(\Delta\sigma(\Delta P))}{dP} \tag{22}$$

3. Experimental Procedure

The tensile tests on the SiC fiber tows were carried out as follows. The test specimens were prepared according to the protocol described in [28,29]. Care was taken during the specimen preparation and tests to avoid specific drawbacks, such as fiber slack [12,16] and friction [15,21]. The bundles were extracted from a spool of fiber. Then, a special support was used for the test specimen preparation. It possessed alignment grooves into which the cylindrical tubes were placed. An untwisted multifilament tow was then introduced into the tubes and stretched and the tow ends were sealed into small-diameter tubes using an adhesive. The tubes were then gripped into the jaws of the testing machine. The gauge length is the inner distance between the tubes.

The tensile tests were carried out at constant cross-head displacement rate of 7.5 mm/min (strain rate 0.1/min). The total elongation was measured by the displacement of the mobile grip (cross-head displacement). The deformation of the load train was subtracted from the total deformation to determine the tow deformation. It was derived from the load train compliance, which was measured on tow specimens with gauges as long as 25, 50, 75, and 100 mm for the tests. Three tests per gauge length were carried out for this purpose.

4. Results

4.1. Load Train Compliance

Figure 4 shows typical examples of the unstable fracture observed on the SiC fiber tows. Note that it occurred close to the theoretical value of maximum force at 1% strain. Figure 5 shows an example of partially stable tensile behavior for a SiC Hi Nicalon fiber tow that displays significant load drop features that reflect multiplet failures. However, it can be noted that the first load drop was the most significant, and it happened at 0.8% strain, as above; see in Figure 4a.

The elastic compliance was measured as the reciprocal of the slope of the force–displacement curves in the linear elastic regime of deformation. Figure 6 shows a typical plot of compliance values as a function of the gauge length. The load train compliance is given by the coordinate of the intercept of the curve with the y-axis. A value of C_{LT} = 0.3 μm/N was obtained on the SiC Nicalon, Hi Nicalon, and Hi Nicalon S fiber tows on the same testing machine for the same specimen preparation protocol.

4.2. Influence of Dominant Factors

The behavior is governed by the competition between the overstress and strength gradient according to Equation (20). The strength gradient is an intrinsic characteristic of the fiber type, which is depicted by the diagram $\Delta\sigma(\Delta P)/\sigma$ vs. n/N_0. In contrast, the overstress depends on the factors λ, n, k, and p. Unstable failure depends on the respective positions of both diagrams of the strength gradient and overstress. Figures 7–9 show diagrams of overstress vs. the strength gradient as a function of the failure probability of

the filaments ($P = n/N_0$). It is worth pointing out that the failure probability allows the identification of filaments using the cumulative strength distribution.

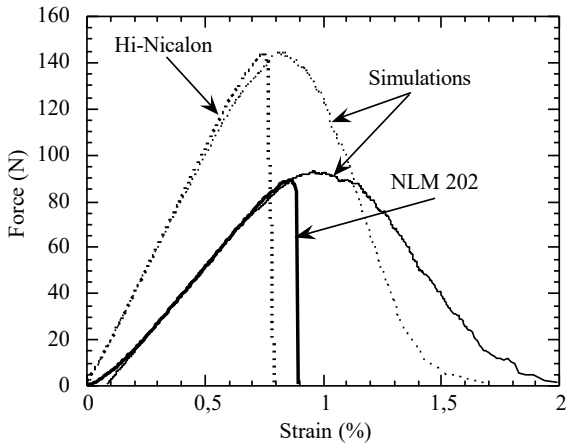

(**a**)

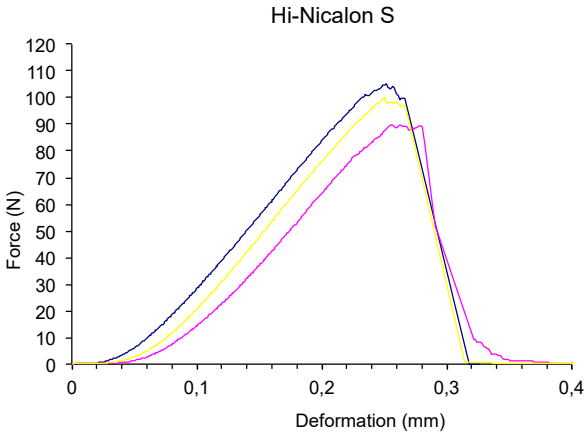

(**b**)

Figure 4. Force–strain curves showing unstable failure of (**a**) SiC Nicalon and Hi Nicalon fiber tows and (**b**) Hi Nicalon S-type fiber tows (L_0 = 25 mm), under strain-controlled loading condition.

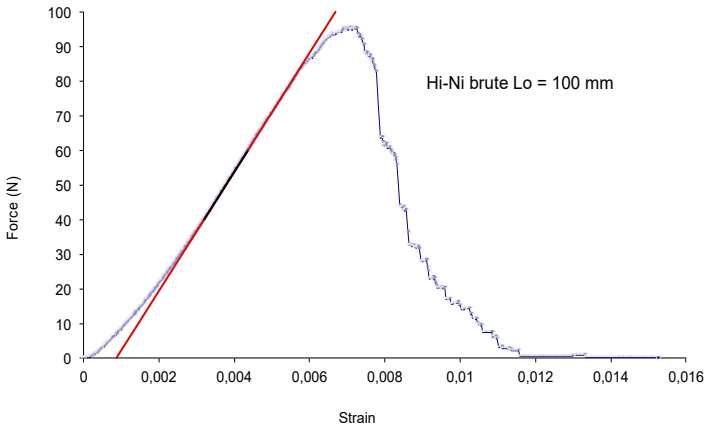

Figure 5. Force–strain curve of Hi Nicalon fiber tow showing features of multiplet failures beyond maximum load.

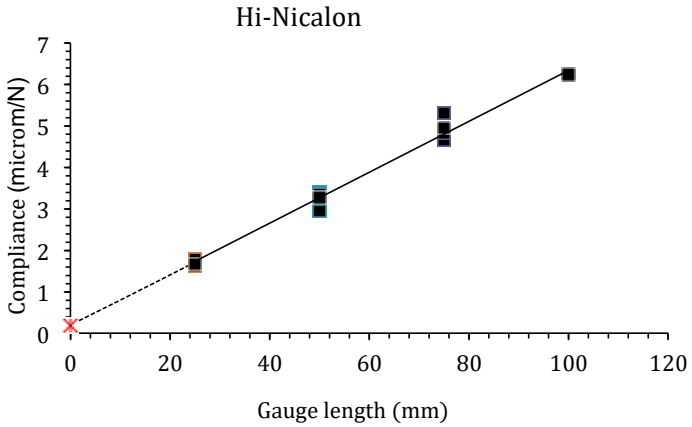

Figure 6. Total compliance versus gauge length measured on Hi Nicalon fiber tow test specimens. $R^2 = 0.9876$, $C_{LT} = 0.3$ µm/N.

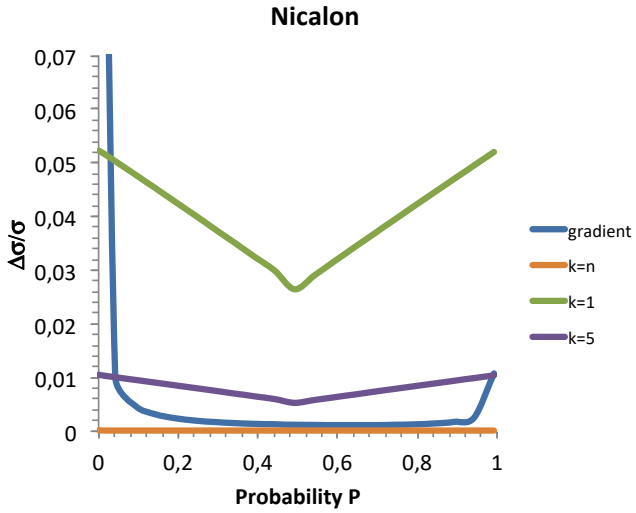

Figure 7. Nicalon: Comparison of overstressing against strength gradient as a function of filament failure probability for various values of k. Gauge length $L_0 = 75$ mm and $\lambda_{exp} = 1.11 \times 10^{-4}$ (Table 1).

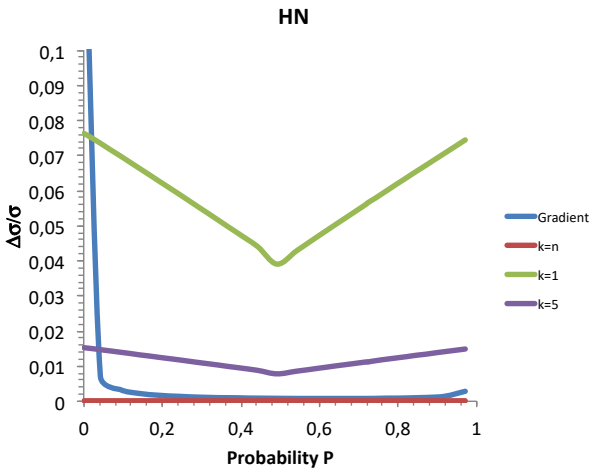

Figure 8. Hi Nicalon: Comparison of overstressing against strength gradient as a function of the filament failure probability for various values of k. Gauge length $L_0 = 75$ mm and $\lambda_{exp} = 1.66 \times 10^{-4}$ (Table 1).

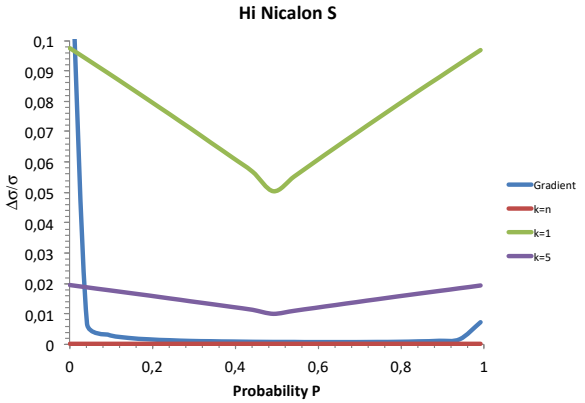

Figure 9. Hi-Nicalon S: Comparison of overstressing against strength gradient as a function of filament failure probability for various values of k. Gauge length L_0 = 75 mm and $\lambda_{exp} = 2.18 \times 10^{-4}$ (Table 1).

Table 1. Characteristics of the loading train and the fibers for the tested SiC tows. r is the filament radius.

	C_{LT} (m/N)	E_f (GPa)	r (μm)	L_0 (mm)	λ_{exp}	N_0
Nicalon	3×10^{-7}	180	7	75 115	1.11×10^{-4} 7.23×10^{-5}	500
Hi-Nicalon	3×10^{-7}	270	7	75 25	1.66×10^{-4} 4.99×10^{-4}	500
Hi-Nicalon S	3×10^{-7}	408	7	75	2.17×10^{-4}	500

4.2.1. Influence of the Number of Filaments Sharing the Overload k

Figures 7–9 show the sensitivity of overstress to k, the number of filaments subjected to overloading. First of all, a comparison of the diagrams indicates that the overstress was smaller for the SiC Nicalon and higher for the Hi Nicalon S fiber tows, whatever k. Then, the strength gradient diagram of Nicalon fiber tows was above that of Hi Nicalon and Hi Nicalon S fiber tows.

It appears from the figures that the intersection of the overstressing and strength gradient curves occurs for $k < n$. The criterion of instability (Equation (2)) is satisfied. For $k = n$, there was no intersection, so the criterion was not satisfied. Thus, large values of k are favorable parameters to avoid unstable failure. Figures 7–9 show that the unstable fracture of the SiC fiber tows is possible for $k < n$ and for the current experimental value λ_{exp}, which agrees with the observed experimental behavior of the dry tows. Furthermore, potential instability requires that the critical filaments are located in the vicinity of the broken fiber. From this point of view, the occurrence of critical overstressing is erratic.

k_c is the minimum number k of filaments for which unstable failure does not occur. Its expression was derived from Equation (21):

$$k_c = \frac{\lambda p(n-p)}{\Gamma(1+\lambda(n-p))} \tag{23}$$

The values of the Weibull modulus for the calculation of Γ are given in Table 2. Figure 10 compares the values of k_c obtained when p = 1 (no inter-fiber friction) for various SiC fiber types. At a given probability, larger values of k_c were obtained for the Hi Nicalon S tows and smaller values for the Nicalon, compared to the Hi Nicalon. This indicates that the Nicalon tows are less sensitive to the phenomenon of overloading from the load train since fewer filaments sharing the overload are necessary to prevent unstability.

The current values of k_c for the failures observed experimentally were estimated for the strain ε_R = 1%. This value was mostly observed on the SiC fiber tows at unstable fracture, as indicated above. It was generally in the area of the maximum of the force–strain curve.

Table 2. Experimental values of k_c, the minimum number of filaments required to prevent instability.

	ε_R (%)	m	σ_0 (MPa)	*Probability P*	k_c
Nicalon	1	4.8	16	0.49	23
Hi Nicalon	1	6.8	61	0.45	49
Hi Nicalon S	1	7.1	99	0.4	63

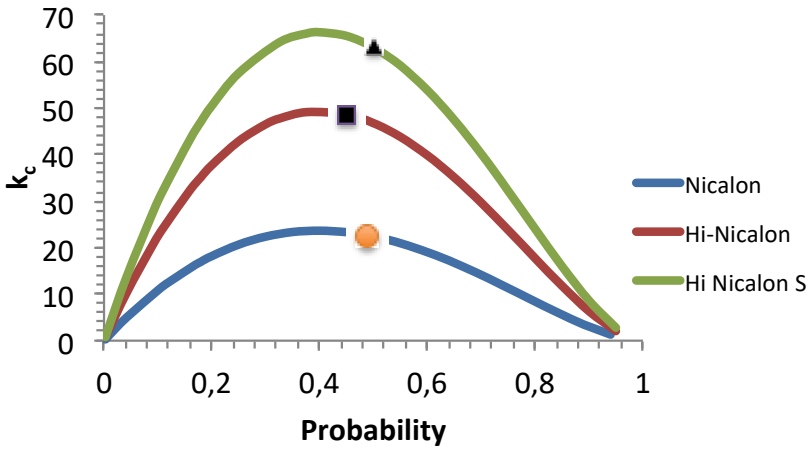

Figure 10. Values of k_c versus filament failure probability, for p = 1 filament. Also indicated are the experimental values estimated at a strain of about 1%, close to maximum force. Gauge length L_0 = 75 mm, $\lambda = \lambda_{exp}$ (Table 1).

The values of probability corresponding to ε_R required for the computation of Γ were obtained using the Weibull Equation (3), for the statistical parameters given in Table 2. $\lambda = \lambda_{exp}$ (Table 1) and L_0 = 75 mm were considered for the analysis.

The current experimental values of k_c are smaller for the SiC Nicalon fiber tows: 23 against 48 and 63 for Hi Nicalon and Hi Nicalon S, respectively (Table 2). They reflect lesser sensitivity to unstable failure, whereas the Hi Nicalon fiber tows displayed intermediate sensitivity, and the Hi-Nicalon S fiber tows displayed higher sensitivity.

4.2.2. Influence of the Size of Multiplets p

Figure 11 shows the influence of the size of the multiplets (p) on k_c, as a function of n, the number of fibers carrying the load. n was derived from the failure probabilities P as $P = (N_0\text{-}n)/N_0$. As expected, it can be seen that k_c increases with the size of the multiplets p. This result reflects that a larger number of filaments is required to share the overload in the presence of bigger multiplets. Table 3 summarizes the particular values of n and k_c extracted from Figure 11 for the SiC Nicalon tows. It shows that there is a critical value of p above which k_c exceeds the number of intact filaments (n-p). In this case, the number of surviving filaments is ineffective to prevent unstable failure of the tows. This critical value of p is 10 filaments.

Table 3. Influence of the size of multiplets p on k_c and the number of surviving filaments (n-p) for Nicalon fiber tows.

ε_R (%)	n	p	k_c	n-p	$(n\text{-}p)/k_c$	Unstability
1	255	1	23	254	>1	probable
1	255	5	111	250	>1	probable
1	255	10	225	245	>1	probable
1	255	11	255	244	<1	certain
1	255	20	419	235	<1	certain

A similar trend was obtained on Hi Nicalon and Hi Nicalon S. The results show that Hi Nicalon S is particularly sensitive to the contribution of multiplet failure to the unstable failure (Figure 12). It is worth pointing out that the critical multiplet size (p = 3; Table 4) is quite small compared to that for SiC Nicalon tows.

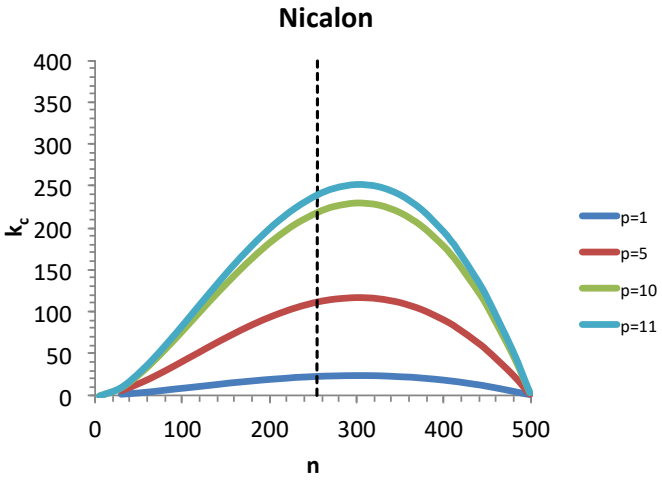

Figure 11. Influence of the size of multiplets (p) on k_c for Nicalon filaments. The vertical dotted line indicates the value of the number of fibers carrying the force (n) at unstable fracture (ε_R = 1%).

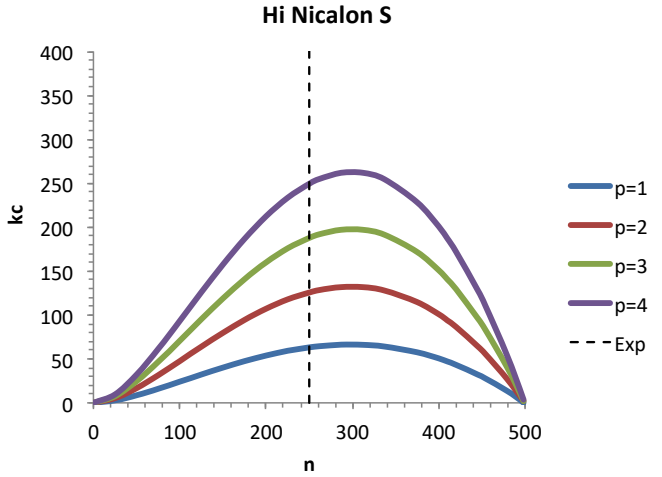

Figure 12. Influence of the size of multiplets (p) on k_c for Hi Nicalon filaments. The vertical dotted line indicates the value of the number of fibers carrying the force (n) at unstable fracture (ε_R = 1%).

Table 4. Influence of the size of multiplets p on k_c, the number of surviving filaments (n-p), for Hi Nicalon S fiber tows.

ε_R (%)	n	p	k_c	n-p	(n-p)/k_c	Unstability
1	250	1	63	249	>1	probable
1	250	2	128	248	>1	probable
1	250	3	190	247	>1	probable
1	250	4	254	246	<1	certain
1	250	20	848	230	<1	certain

4.2.3. Influence of λ and Gauge Length L_0

Figure 13 shows that the overstressing decreases with λ whatever the gauge length, and that it is smaller than the stress gradient for $\lambda_1 < \lambda_2$ (Table 5). Small values of λ are appropriate parameters to avoid unstable failure.

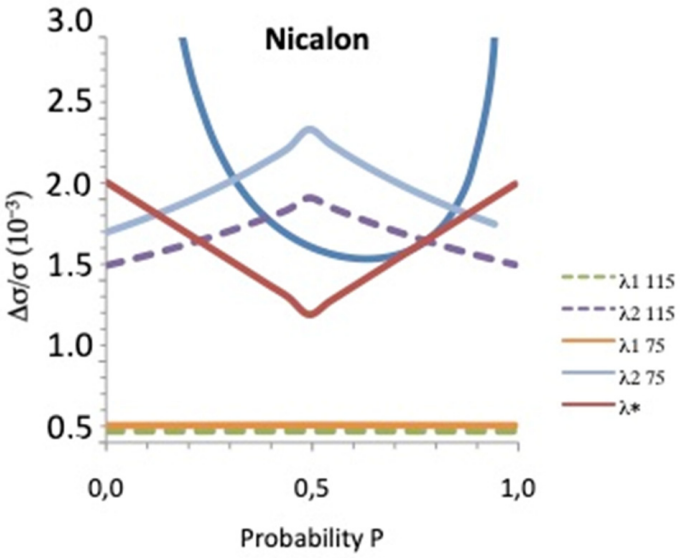

Figure 13. Comparison of overstressing against strength gradient for $k = n$, $\lambda_1 < \lambda_2$ (Table 5), $p = 1$ and gauge lengths of 75 and 115 mm. Also shown is the tangent critical overstressing curve for the critical value λ^*.

Table 5. Values of λ used for the predictions shown on Figure 13 for SiC Nicalon.

	C_{LT} (m/N)	λ (L_0 = 75 mm)	λ (L_0 = 115 mm)
λ_1	3.0×10^{-7}	1.11×10^{-4}	7.23×10^{-5}
λ_2	10^{-5}	3.69×10^{-3}	2.41×10^{-3}

The same trend was obtained on the Hi Nicalon and the Hi Nicalon S fiber tows.

Critical Value of λ^*

The critical value λ^* below which there is no contribution of the load train deformation whatever the values of n, p and k is that value at which the overstressing curve is tangent to the gradient curve, as depicted in Figures 13 and 14. It was determined from Equations (19) and (22) for the worst case defined by $k = 1$, i.e., the overload being concentrated on a single filament, and for $p = 1$ filament (no multiplet). Table 6 shows that λ^* decreases when p increases. The values of λ^* for the SiC fibers in this study are given in Table 6. Note that Hi Nicalon and Hi Nicalon S are quite close, whereas Nicalon appears to be less sensitive to overstressing owing to a higher strength gradient. Note that $\lambda_{exp} > \lambda^*$ (Table 6), which indicates that the probability of unstable failure of the SiC tows in this paper was >0.

Figure 15 shows the decrease in λ with an increasing gauge length, according to Equation (13). The Hi Nicalon S tows display the largest values of λ whatever the gauge length. The theoretical critical gauge lengths at which one would not observe unstable failure were derived from the critical values λ^* (Table 6). Note that they are quite large (Table 6): >2 m for Nicalon, >5 m for Hi Nicalon, and 8 m for Hi Nicalon S. As expected from the previous results, all these results confirm the ranking of sensitivity to unstable failure due to overstressing: Nicalon tows are the least sensitive while the Hi Nicalon S tows are the most sensitive. This is related to the difference in the filaments' Young's modulus. It can be anticipated that at such large gauge lengths, the inter-fiber friction would be enhanced if an appropriate lubricant were not used. Furthermore, testing tows of such sizes will present practical difficulties.

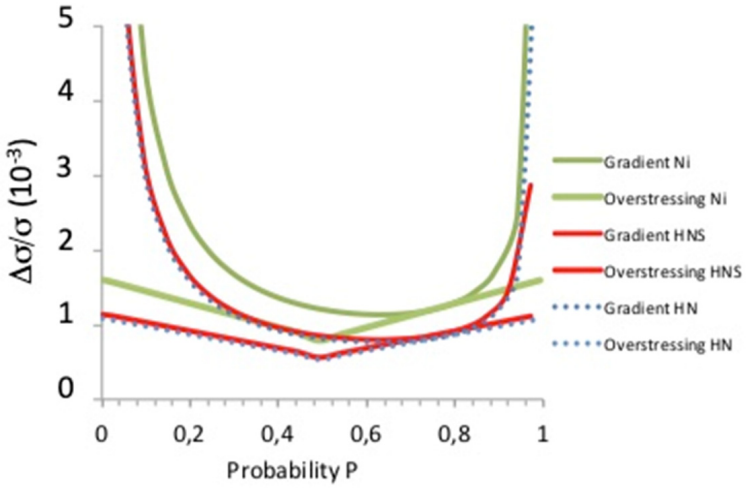

Figure 14. Overstressing against strength gradient for $k = 1$, $p = 1$, λ^* (Table 6), and gauge length of 75 mm.

Table 6. Values of λ^* for $k = 1$, $L_0 = 75$ mm, and various values of p. Also indicated are the values of λ_{exp} and the values of critical gauge length $L_0{}^*$.

p	*Nicalon*	*Hi Nicalon S*	*Hi Nicalon*
1	3.23×10^{-6}	2.18×10^{-6}	2.3×10^{-6}
2	1.60×10^{-6}	1.10×10^{-6}	
3		7.50×10^{-7}	
4		5.50×10^{-7}	
5	6.50×10^{-7}		
10	3.30×10^{-7}		
λ_{exp}	1.11×10^{-4}	2.17×10^{-4}	1.66×10^{-4}
$L_0{}^*$ (m)	2.57	8.65	5.41

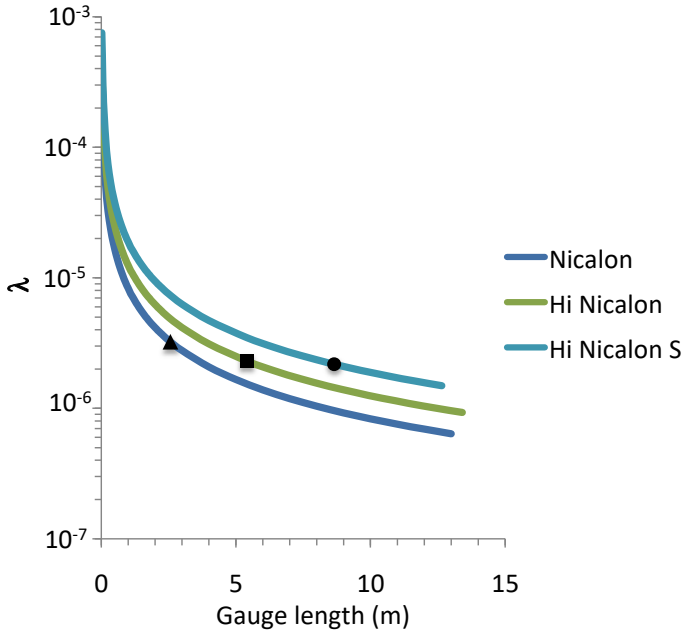

Figure 15. Influence of gauge length on λ for the C_{LT} value of the present study (3×10^{-7} m/N). Also shown are the critical values of gauge lengths corresponding to λ^*.

5. Discussion

The analysis of the influence of the main parameters λ, n, k, p, and L_0 converge toward the conclusion that unstable fracture from overstressing was possible under the experimental conditions characterized by the value of λ_{exp} in this paper. The main condition of stability $\lambda_{exp} < \lambda^*$ was not fulfilled. The second one, $k > k^*$, is erratic, as well as the third one, $p > p^*$.

It appears that the Hi Nicalon S fiber tows present the greatest sensitivity to overloading compared to Hi Nicalon and then to Nicalon. This agrees with the common observations of unstable failure, which was frequent for Hi Nicalon S and to a lesser extent for Hi Nicalon, in contrast to Nicalon.

The reduction in sensitivity to overloading requires $\lambda < \lambda^*$, $k > k^*$ (for sharing of overload), $p = 1$ (no multiplet failure). Small values of λ require small values of load train compliance (high stiffness) and the large gauge length of the tow. Stiff fibers like Hi Nicalon S lead to large λ, so a large gauge length L_0 should be selected for these fibers. Whether C_{LT} can be adjusted is not certain, as it depends on the adhesive properties and bonding of the tow ends to the tabs. The displacement within the adhesive that had been used to attach the bundles to the tabs should be reduced. p can be reduced to 1 filament by using a lubricant to prevent friction due to inter-fiber contact. It seems that the same requirements as before for C_{LT} should be met to control k the number of filaments that share the overload. A sound solution seems to be the technique using long thermoretractable rings that are threaded onto the bundle ends [14] close to the grips. As exemplified by Figure 1, a great number of force–strain curves obtained with this technique show a smooth controlled load decrease beyond the maximum (Figure 1) [9]. It may be thought that the load train compliance was comparable to the present paper because the tow ends were also bonded to the tubes using resin [14]. Therefore, it can be inferred that the thermoretractable rings allowed a large number of filaments ($k > k^*$) to share the extra load generated by the elastic deformation of the load train. This would reduce, if any, the overstress on the filaments.

In the common technique [28,29], the regions outside the fiber specimen gauge length are bonded to plates (aluminum or epoxy) or tubes. It seems highly probable that the load train deformation was not uniform and that the overload was concentrated on a few filaments, leading to small k. This agrees with the high frequency of occurrence of tow unstable failures. The number of filaments that carry the overload is erratic. There is no closed-form equation to predict the criticality of the reaction of the load train. The solution to reduce the chances of unstable fracture is to use the technique with thermoretractable rings [14] together with controlling λ, which implies adjustment of the load train compliance and gauge length.

When non-critical, the extra load may lead to an underestimation of strength. This effect was not estimated in the present paper due to space and time constraints, and it was thought that it fell out of scope. However, a lower bound of the possible strength can be calculated using the model of overloading, and the strength gradient. Underestimated strengths are prudent estimates but they lead to a higher value of the Weibull modulus.

It is worth pointing out that the force–strain curve of SiC Nicalon shown in Figure 1 was found to agree with the results of the single-filament tensile tests [9]. Thus, the cumulative distribution function of the filament strengths derived from the tests on the tows fitted well with that derived from the single-filament tensile tests [9]. This suggests that the effect of the load train was negligible when thermoretractable rings were used.

The meaning of the stress at the unstable fracture of tows and the distribution that might be associated is an issue under strain-controlled load conditions. This failure is caused by the uncontrolled overload from the reaction of the load train. It is governed by extraneous factors such as the number of filaments that carry the overload (k) and the size of possible multiplets (p) instead of the flaw population. The occurrences of k and p are erratic events. Therefore, the corresponding stress on the tow does not measure the tow's strength, and the variability cannot be characterized using the Weibull distribution. These results agree with previous results that show that the value of maximum force should not

be scattered when the number of filaments in the tow is large [16,24,30,31]. The true tow strength under strain-controlled conditions is given by the strength of the strongest filament. Under force-controlled conditions, it is given by the critical filament at the maximum force.

6. Conclusions

A quantitative approach to evaluating the quality of tensile tests on dry tows and to designing the proper test conditions was proposed in the present paper. The critical factors that govern the unstable failure of tows were identified and quantified. The phenomenon of overloading from the reaction of the load train when a filament fails was assessed. Unstable failure is governed by the balance between overstress and the filament strength gradient. This phenomenon allows us to solve the apparent inconsistency in the unstable failure under strain-controlled conditions of loading when force relaxation operates. Under strain-controlled conditions, there is theoretically no overloading from the failure of a filament. Ultimate failure should result from the failure of the strongest filament in the tow. The contribution of inter-fiber friction stress, which may enhance the phenomenon, was introduced into the model.

The unstable failure of tows was shown to depend on the following factors: the intrinsic sensitivity coefficient λ that characterizes the load train–test specimen couple, the number of filaments carrying the applied load (n), the number of filaments sharing the overstress (k), and the number of filaments failing from the overstress due to inter-fiber friction (p). To avoid unstable failure, λ should be smaller than the critical value λ^*, k should be larger than the critical value k_c, and the gauge length should be larger than the critical length L_0^*. Critical values of these factors were determined for the SiC fiber tows and for the tow–load train couple in this paper. This approach allows us to design the proper conditions for other systems. The Hi Nicalon S was the most sensitive to overloading. In contrast, the Hi Nicalon fiber tows exhibited intermediate sensitivity, and the Nicalon the lowest sensitivity. This ranking was consistent with the experimental observations reported by various experimenters.

The technique devised in [15] affords a sound way to avoid unstable failure. It used an extensometer clamped to the specimen using two 4 mm long thermoretractable rings positioned at the end of the test specimen, close to the grips. This system is thought to generate global sharing of the overload (k close to n), which reduced the probability of unstable failure. Unstable failure was not observed when using the technique, except on Hi Nicalon S fiber tows.

Unstable failure of the dry tows does not correspond the tow strength. Fracture does not result only from the boundary conditions of loading and the population of fracture-inducing flaws but also from an extra load. The tow strength is dictated by the critical filament, which depends on the loading mode (balance between force and strain control) and local stress state. This variability results from the variability in n, k, and p. The variation in these parameters is erratic but not stochastic. As such, it cannot be described by a formal law. Therefore, the corresponding stress cannot be mixed up with the tow strength, and variability cannot be characterized using the Weibull distribution.

Funding: This research received no external funding.

Data Availability Statement: The data can be shared upon request.

Acknowledgments: The author thanks the former PhD students who carried out the tests on the tows at LCTS (the Laboratory of Thermostructural Composites, the University of Bordeaux, CNRS, CEA, and Safran).

Conflicts of Interest: The author declares no conflicts of interest.

References

1. Bunsell, A. (Ed.) *Handbook of Properties of Textile and Technical Fibers*, 2nd ed.; Elsevier: Amsterdam, The Netherlands, 2018; ISBN 9780081012727.
2. Duan, Y.; Chen, X.; Yin, B.; Zhao, X.; Zhao, Z.; Hou, B.; Li, Y. Understanding the effect of defects on compressive behaviors of closed-cell foams: Experiment and statistical model. *Compos. Part B Eng.* **2022**, *244*, 110179. [CrossRef]
3. Xu, L.; Zhang, R.; Niu, L.; Qi, C. Damage Model of Basalt-Fiber-Reinforced Cemented Soil Based on the Weibull Distribution. *Buildings* **2023**, *13*, 460. [CrossRef]
4. Bergman, B. On the estimation of the Weibull modulus. *J. Mater. Sci. Lett.* **1984**, *3*, 689–692. [CrossRef]
5. Davies, I.J. Best estimate of Weibull modulus obtained using linear least squares analysis: An improved empirical correction factor. *J. Mater. Sci.* **2004**, *39*, 1441–1444. [CrossRef]
6. Griggs, J.A.; Zhang, Y. Determining the confidence intervals of Weibull parameters estimated using a more precise probability estimator. *J. Mater. Sci. Lett.* **2003**, *22*, 1771–1773. [CrossRef]
7. Lamon, J.; R'Mili, M.; Reveron, H. Investigation of statistical distributions of fracture strengths for flax fibre using the tow-based approach. *J. Mat. Sci.* **2016**, *51*, 8687–8698. [CrossRef]
8. R'Mili, M.; Godin, N.; Lamon, J. Flaw strength distributions and statistical parameters for ceramic fibres: The Normal distribution. *Phys. Rev. E* **2012**, *85*, 1106–1112.
9. Lamon, J.; R'Mili, M. Investigation of flaw strength distributions from tensile force-strain curves of fiber tows. *Compos. Part A* **2021**, *145*, 106262. [CrossRef]
10. Coleman, B.D. On the strength of classical fibers and fibers bundle. *J. Mech. Phys. Solids* **1958**, *7*, 60–70. [CrossRef]
11. Chi, Z.; Wei Chou, T.; Shen, G. Determination of single fiber strength distribution from fiber bundle testing. *J. Mat. Sci.* **1984**, *19*, 3319–3324. [CrossRef]
12. Phoenix, S.L. Probabilistic strength analysis of fiber bundles structures. *Fibre Sci. Technol.* **1974**, *7*, 15–31. [CrossRef]
13. Creasy, T.S. Modeling analysis of tensile tests of bundled filaments with a bimodal Weibull survival function. *J. Comp. Mat.* **2002**, *36*, 183–194. [CrossRef]
14. R'Mili, M.; Murat, M. Caractérisation des fibres par amélioration de l'essai sur mèche avec mesure directe de la déformation. *C. R. Acad. Sci.* **1989**, *314*, 355–364. [CrossRef]
15. R'Mili, M.; Moevus, M.; Godin, N. Statistical fracture of E-glass fibres using a bundle test and acoustic emission monitoring. *Comp. Sci. Technol.* **2008**, *68*, 1800–1808. [CrossRef]
16. Calard, V.; Lamon, J. Failure of fibres bundles. *Compos. Sci. Technol.* **2004**, *64*, 701–710. [CrossRef]
17. R'Mili, M.; Bouchaour, T.; Merle, P. Estimation of Weibull parameters from loose bundle tests. *Comp. Sci. Technol.* **1996**, *56*, 831–834. [CrossRef]
18. Yun, H.M.; Di Carlo, J.A. Thermomechanical behavior of advanced SiC fiber multifilament tows. *Ceram. Eng. Sci. Proc.* **1996**, *17*, 61–67.
19. Dassios, K.G.; Steen, M.; Filiou, C. Mechanical properties of alumina NextelTM 720 fibres at room and elevated temperatures: Tensile bundle testing. *Mater. Sci. Eng. A* **2003**, *349*, 63–72. [CrossRef]
20. Lamon, J.; R'Mili, M. Stochastic approach to the lifetime and strength degradation of E-glass filaments and bundles under constant loading in water, Special Issue Durability of Composites Under Severe Environmental Conditions. *J. Compos. Sci.* **2019**, *3*, 78. [CrossRef]
21. Hill, R.; Okoroador, E.U. Weibull statistics of fibre bundle failure using mechanical and acoustic emission testing: The influence of interfibre friction. *Composites* **1995**, *26*, 699–705. [CrossRef]
22. Callaway, E.B.; Zok, F.W. Strengths of ceramic fiber bundles: Theory and practice. *J. Am. Ceram. Soc.* **2017**, *100*, 5306–5317. [CrossRef]
23. Peirce, F.T. Tensile tests for cotton yarns vs "the weakest link". *J. Text. Inst.* **1926**, *17*, 355.
24. Daniels, H.E. The Statistical Theory of the Strength of Bundles of Threads. I. *Proc. R. Soc. A Math. Phys. Eng. Sci.* **1945**, *183*, 405–435.
25. Hamstadt, M.A.; Moore, R.L. Acoustic emission from single and multiple Kevlar 49 filament breaks. *J. Comp. Mater.* **1986**, *20*, 46–66. [CrossRef]
26. Stoner, E.G.; Edie, D.D.; Durham, S.D. An end-effect model for the single filament tensile test. *J. Mat. Sci.* **1994**, *29*, 6561–6574. [CrossRef]
27. Weibull, W. A statistical theory of the strength of materials. *R. Swed. Inst. Eng. Res.* **1939**, *151*, 1–45.
28. *European standard EN 1007-5*; Advanced Technical Ceramics—Ceramic Composites—Methods of Test for Reinforcements-Part 5: Determination of Distribution of Tensile Strengths and of Tensile Strains to Failure of Filaments within a Multifilament Tow at Ambient Temperature. Comité Européen de Normalisation: Bruxelles, Switzerland, 1998.
29. *ISO 22459*; Fine Ceramics (Advanced Ceramics, Advanced Technical Ceramics)—Methods of Test for Reinforcements—Determination of Distribution of Tensile Strength and of Tensile Strain to Failure of Filaments within a Multifilament Tow at Ambient Temperature. International Standard Organisation: Geneva, Switzerland, 2020.

30. McCartney, L.N.; Smith, R.L. Statistical theory of the strength of fiber bundles. *ASME J. Appl. Mech.* **1983**, *105*, 601–608. [CrossRef]
31. Gurvich, M.; Pipes, R. Strength size effect of laminated composites. *Comp. Sci. Technol.* **1995**, *55*, 93–105. [CrossRef]